第 35 卷第 6 期 无 机 化 学 学 报 Vol.35 No.6
2019 年 6 月 CHINESE JOURNAL OF INORGANIC CHEMISTRY 1093-1100

一个含 1-甲基咪唑的环状梯型核$[V_{10}O_{20}]$及特别的电子构型的十核钒氧簇合物的合成、结构及理论计算

童义平*,[1,2] 郑晓丹[1,2] 李佳佳[1,2] 林燕文[3] 罗国添*,[4]
([1]惠州学院化学与材料工程学院,惠州 516007)
([2]广东高校绿色化工与功能材料工程技术开发中心,惠州 516007)
([3]惠州学院生命科学学院,惠州 516007)
([4]赣南师范大学化学化工,赣州 341000)

摘要:合成并表征了一个稀少的含 1-甲基咪唑(L)及混合价的$[V_{14}O_{36}F_2L_2]^{6-}$阴离子化合物的晶体结构。该阴离子是由一个环状的$[V_{10}O_{20}]$梯和 2 对架于梯上的 VO_5F 及 VO_3L 碎片组成。DFT 及键价计算表明架着的 VO_5F 碎片中 V 是+4 价,其余 V 均为+5 价。前线分子轨道分析表明:$[V_{14}O_{36}F_2L_2]^{6-}$阴离子架着的 VO_5F 碎片中,V 的 *d* 轨道是化学上活性的;而其 2e 氧化型$[V_{14}O_{36}F_2L_2]^{4-}$阴离子的 VO_3L 碎片中,端基 V=O(*d-p*) π 轨道是化学上活性的。从$[V_{14}O_{36}F_2L_2]^{4-}$变成$[V_{14}O_{36}F_2L_2]^{6-}$阴离子,2e 的引入,导致了$[V_{10}O_{20}]$梯更加稳固,但架于其上的 VO_5F 及 VO_3L 碎片却越来越活泼(不稳定),并且能隙大幅降低(从 1.59 eV 变为 0.53 eV)。

关键词:聚钒氧酸盐;DFT 计算;梯型;能隙;分子碎片;1-甲基咪唑
中图分类号:O614.51+1 **文献标识码**:A **文章编号**:1001-4861(2019)06-1093-08
DOI:10.11862/CJIC.2019.121

A Tetradecanuclear Polyoxofluorovanadate Cluster Compound with 1-Methylimidazole Possessing Ring-like $[V_{10}O_{20}]$ Ladder Core and Unusual Electronic Configuration: Synthesis, Structure and Theoretical Calculation

TONG Yi-Ping*,[1,2] ZHENG Xiao-Dan[1,2] LI Jia-Jia[1,2] LIN Yan-Wen[3] LUO Guo-Tian*,[4]
([1]*School of Chemistry and Materials Engineering, Huizhou University, Huizhou, Guangdong* 516007, *China*)
([2]*Center of Green Chemical Engineering and Functional Materials of Guangdong Provincial Universities, Huizhou, Guangdong* 516007, *China*)
([3]*School of Life Science, Huizhou University, Huizhou, Guangdong* 516007, *China*)
([4]*College of Chemistry and Life Science, Gannan Normal University, Ganzhou, Jiangxi* 341000, *China*)

Abstract: A rare tetradecanuclear polyoxofluorovanadate cluster with 1-methylimidazole (L), containing mixed-valence $[V_{14}O_{36}F_2L_2]^{6-}$ anion, was synthesized and characterized crystallographically. The anion is composed of a special 0D cluster-like skeleton frame, *i.e.* the ring-shaped $[V_{10}O_{20}]$ ladder, two grafted VO_5F and VO_3L fragments around the ladder. The density functional theory (DFT) and bond valence sum calculations indicate that the V ion in two grafted VO_5F fragments are +4 oxidation state, while other V ions are +5 oxidation state. The frontier orbital analysis shows that the $[V_{14}O_{36}F_2L_2]^{6-}$ anion, should be chemically active in *d* orbital of grafted VO_5F fragments, while its 2e oxidation species, the $[V_{14}O_{36}F_2L_2]^{4-}$ anion should be chemically active in the terminal V=O (*d-p*) π orbital of grafted VO_3L fragments. The 2e introduction from $[V_{14}O_{36}F_2L_2]^{4-}$ to $[V_{14}O_{36}F_2L_2]^{6-}$ anion leads to

收稿日期:2019-01-04。收修改稿日期:2019-03-25。
广东省普通高校创新团队项目无机固体功能材料研究团队(No.2015KCXTD030),国家自然科学基金(No.21271080),广东高校绿色化工与功能材料工程技术开发中心建设项目及惠州市科技计划项目(No.2012B020004006)资助。
*通信联系人。E-mail:typ2469@163.com

the increasing structural stability of the $[V_{10}O_{20}]$ ladder, and at the same time the increasing chemical activity of the grafted VO_5F and VO_3L fragments, together with a great decrease of energy gap from 1.59 to 0.53 eV. CCDC: 761054.

Keywords: polyoxofluorovanadate; DFT calculation; ladder-like; energy gap; molecular fragment; 1-methylimidazole

0 Introduction

Polyoxometalates with oxygen/fluorine donor groups show an impressive structural and electronic diversity in the past few years[1-7], and extensive synthetic research has been carried out in this field[8-11]. As a result, a large number of novel compounds with cluster-like anionic structures have been reported previously. These novel anionic polyoxometalate structures may be spherical, basket-shaped, half-spherical, bowl-shaped and so on, which show application potentials in catalytic, magnetic, optical, electroconductive, and molecular adsorption materials, as well as their interesting structural features[12-17].

However, the tunable synthesis and relative design for these structures are still a challenge for inorganic chemists. The synthetic routines for these compounds are quite diversiform. For example, some spherical polyoxometates have been obtained by capping guest molecule and assembling into the half-spherical or bowl-type molecule, *etc*, and gradually completing the sphere; some obtained by using cations as structure directing agents, in order to develop novel structural building units, and direct towards the rational synthesis of novel polyoxometalate.

We and other groups have made a series of compounds featuring different polyoxofluorovanadate anionic clusters of zero-dimensional (0D), one-dimensional (1D) and two-dimensional (2D) structures[1,18-20], with different metal counter ions, e.g. K(Ⅰ), Ca(Ⅱ) and Sr(Ⅱ), an indicative that the counter cations may effectively tune the formation of polyoxofluorovanadate anionic clusters. Similar observations have been also available in other anionic metal clusters with oxygen/sulphur donor groups when organic cations being counter ions in the past. Herein we report a rare structure of V_{14}-based polyoxofluorovanadate anionic cluster, containing both coordinative methylimidazole and protonated methylimidazole cations, *i.e.* $(HL)_6[V_{14}O_{36}F_2L_2]\cdot 4H_2O$ (**1**, L=1-methylimidazole), together with a theoretical investigation of electronic structure, possible information mechanism, and structure-property relationship analysis.

1 Experimental

1.1 Synthesis

Compound **1** was obtained by a reaction of V_2O_5 (0.091 g, 0.5 mmol), L (0.494 g, 6 mmol), and HF (*ca.* 30%, *w*/*w*) in an aqueous solution of 1.25 mL. The mixture was heated in Teflon-lined steel autoclaves with an inner volume of 23 mL for one day at 155 ℃ and then cooled to room temperature at a speed of 5 ℃·h^{-1}. After washing with water and acetone, dried at room temperature, black green crystals were obtained. The compound is stable on air and in water. Yield: *ca.* 40%. Anal. Calcd. for $C_{32}H_{62}F_2N_{16}O_{40}V_{14}$(%): C 18.64, H 3.03, N 10.87; Found(%): C 18.78, H 3.11, N 10.80. FTIR (KBr, cm^{-1}): 3 750 (m), 2 998 (m), 2 558 (m), 2 337 (s), 2 204 (m), 2 070 (w), 1 890 (s), 1 772 (s), 1 583 (m), 1 348 (w), 1 276 (w), 1 233 (w), 924 (m), 839 (s), 687 (w), 485 (w).

1.2 X-ray analysis

A crystal of **1** with dimension of 0.48 mm×0.29 mm×0.20 mm was mounted on glass rod for determining crystal structure. X-ray diffraction measurement was performed on a Bruker SMART-CCD diffractometer with graphite-monochromated Mo $K\alpha$ (λ=0.071 073 nm) radiation in the ω scanning mode at 20 ℃. The SADABS program was used for the absorption correction[21], and the direct method was adopted to solve and refine the structure based on F^2 by full-matrix least-squares techniques using the SHELXTL 97 program package[22]. All of the non-hydrogen atoms were refined anisotropically, and the hydrogen atoms

of the organic ligands were geometrically placed and refined using a riding model. The hydrogen atoms attached to lattice water were located from the different Fourier maps. The final refinement leads to a satisfactory result of R_1 0.045 8, wR_2 0.132 4, and the goodness-of-fit 1.027. Experimental details of the X-ray determination and major geometrical parameters of **1** are presented in Table 1 and 2, respectively.

CCDC: 761054.

Table 1　Crystal data and structure refinement for 1

Empirical formula	$C_{32}H_{62}F_2N_{16}O_{40}V_{14}$	θ range for data collection / (°)	2.25~27.50
Formula weight	2 062.14	Index ranges	$-18 \leqslant h \leqslant 17$; $-16 \leqslant k \leqslant 16$; $-24 \leqslant l \leqslant 25$
Crystal system	Monoclinic	Total reflection	23 797
Space group	$P2_1/c$	Unique reflections (R_{int})	7 564 (0.040 6)
a / nm	1.389 73(12)	Completeness to θ_{max}	96.8
b / nm	1.281 36(11)	Observed data, restraint, parameter	7 564, 6, 485
c / nm	1.998 84(18)	S on F^2	1.027
β / (°)	107.141(1)	R_1[a] [$I>2\sigma(I)$]	0.045 8
V / nm^3	3.401 3(5)	wR_2[b] (all data)	0.132 4
Z	2	Largest difference peak and hole / (e·nm^{-3})	786 and −626
μ / mm^{-1}	1.936		

[a] $R_1=\sum||F_o|-|F_c||/\sum|F_o|$; [b] $wR_2=[\sum w(F_o^2-F_c^2)^2/\sum w(F_o^2)^2]^{1/2}$.

Table 2　Selected bond lengths (nm) and bond angles (°) for 1

V(1)-O(8)	0.160 5(3)	V(3)-O(7)#1	0.193 8(2)	V(6)-O(14)	0.172 2(3)
V(1)-O(9)	0.174 2(3)	V(3)-O(4)	0.199 7(2)	V(6)-O(7)	0.180 3(2)
V(1)-O(3)	0.194 2(3)	V(3)-V(4)	0.305 2(1)	V(6)-O(2)	0.180 5(2)
V(1)-O(5)	0.194 8(2)	V(4)-O(12)	0.161 0(2)	V(6)-O(5)	0.243 3(3)
V(1)-O(2)	0.207 5(2)	V(4)-O(6)	0.171 1(2)	V(7)-O(18)	0.162 3(3)
V(1)-F(1)	0.219 3(2)	V(4)-O(4)	0.191 5(2)	V(7)-O(19)	0.162 9(3)
V(2)-O(17)	0.159 5(3)	V(4)-O(2)	0.193 5(2)	V(7)-O(14)	0.199 1(3)
V(2)-O(16)	0.172 6(3)	V(4)-O(3)	0.200 8(2)	V(7)-O(5)	0.200 8(2)
V(2)-O(4)	0.193 4(2)	V(5)-O(15)	0.161 0(3)	V(7)-N(1)	0.212 4(4)
V(2)-O(5)#1	0.197 7(2)	V(5)-O(6)#1	0.193 3(3)	F(1)-V(2)#1	0.222 8(2)
V(2)-O(7)#1	0.209 4(2)	V(5)-O(13)	0.194 4(3)	O(5)-V(2)#1	0.197 7(2)
V(2)-F(1)#1	0.222 8(2)	V(5)-O(16)#1	0.196 5(3)	O(6)-V(5)#1	0.193 3(3)
V(3)-O(11)	0.161 2(2)	V(5)-O(9)	0.197 7(3)	O(7)-V(3)#1	0.193 8(2)
V(3)-O(13)	0.171 5(3)	V(5)-F(1)	0.221 5(2)	O(7)-V(2)#1	0.209 4(2)
V(3)-O(3)	0.191 8(2)	V(6)-O(10)	0.160 7(3)	O(16)-V(5)#1	0.196 5(3)
O(8)-V(1)-O(9)	102.79(13)	O(11)-V(3)-O(3)	105.17(12)	O(13)-V(5)-O(16)#1	156.21(11)
O(8)-V(1)-O(3)	101.76(13)	O(13)-V(3)-O(3)	96.08(11)	O(15)-V(5)-O(9)	101.80(13)
O(9)-V(1)-O(3)	97.24(11)	O(11)-V(3)-O(7)#1	104.93(12)	O(6)#1-V(5)-O(9)	155.94(11)
O(8)-V(1)-O(5)	102.43(12)	O(13)-V(3)-O(7)#1	94.21(11)	O(13)-V(5)-O(9)	84.25(11)
O(9)-V(1)-O(5)	97.51(12)	O(3)-V(3)-O(7)#1	143.99(11)	O(16)#1-V(5)-O(9)	85.30(11)
O(3)-V(1)-O(5)	147.99(11)	O(11)-V(3)-O(4)	103.59(12)	O(15)-V(5)-F(1)	176.07(13)
O(8)-V(1)-O(2)	96.78(12)	O(13)-V(3)-O(4)	150.41(11)	O(6)#1-V(5)-F(1)	81.35(9)
O(9)-V(1)-O(2)	160.21(11)	O(3)-V(3)-O(4)	76.37(10)	O(13)-V(5)-F(1)	81.48(9)
O(3)-V(1)-O(2)	75.65(10)	O(7)#1-V(3)-O(4)	77.73(10)	O(16)#1-V(5)-F(1)	75.19(9)
O(5)-V(1)-O(2)	80.95(10)	O(11)-V(3)-V(4)	116.44(10)	O(9)-V(5)-F(1)	75.01(9)

Continued Table 1

O(8)-V(1)-F(1)	176.73(11)	O(13)-V(3)-V(4)	123.99(8)	O(10)-V(6)-O(14)	104.51(14)
O(9)-V(1)-F(1)	80.23(10)	O(7)#1-V(3)-V(4)	107.48(7)	O(10)-V(6)-O(7)	106.10(13)
O(3)-V(1)-F(1)	78.98(9)	O(12)-V(4)-O(6)	105.49(13)	O(14)-V(6)-O(7)	114.45(13)
O(5)-V(1)-F(1)	75.76(9)	O(12)-V(4)-O(4)	106.96(12)	O(10)-V(6)-O(2)	105.87(13)
O(2)-V(1)-F(1)	80.29(8)	O(6)-V(4)-O(4)	95.64(11)	O(14)-V(6)-O(2)	111.28(12)
O(17)-V(2)-O(16)	103.34(14)	O(12)-V(4)-O(2)	104.13(12)	O(7)-V(6)-O(2)	113.66(11)
O(17)-V(2)-O(4)	102.74(13)	O(6)-V(4)-O(2)	94.34(11)	O(10)-V(6)-O(5)	178.50(12)
O(16)-V(2)-O(4)	97.92(11)	O(4)-V(4)-O(2)	143.33(11)	O(14)-V(6)-O(5)	74.03(11)
O(17)-V(2)-O(5)#1	102.50(13)	O(12)-V(4)-O(3)	105.04(12)	O(7)-V(6)-O(5)	74.96(10)
O(16)-V(2)-O(5)#1	96.75(11)	O(6)-V(4)-O(3)	149.46(11)	O(2)-V(6)-O(5)	74.49(10)
O(4)-V(2)-O(5)#1	146.88(11)	O(4)-V(4)-O(3)	76.18(10)	O(18)-V(7)-O(19)	109.36(17)
O(17)-V(2)-O(7)#1	97.49(13)	O(2)-V(4)-O(3)	77.40(10)	O(18)-V(7)-O(14)	100.18(15)
O(16)-V(2)-O(7)#1	159.09(11)	O(12)-V(4)-V(3)	118.50(10)	O(19)-V(7)-O(14)	95.21(15)
O(4)-V(2)-O(7)#1	75.49(10)	O(6)-V(4)-V(3)	122.94(8)	O(18)-V(7)-O(5)	118.14(14)
O(5)#1-V(2)-O(7)#1	80.27(10)	O(2)-V(4)-V(3)	107.18(7)	O(19)-V(7)-O(5)	132.41(14)
O(17)-V(2)-F(1)#1	176.12(12)	O(15)-V(5)-O(6)#1	101.63(13)	O(14)-V(7)-O(5)	79.80(11)
O(16)-V(2)-F(1)#1	79.52(10)	O(15)-V(5)-O(13)	100.59(14)	O(18)-V(7)-N(1)	96.89(17)
O(4)-V(2)-F(1)#1	79.30(9)	O(6)#1-V(5)-O(13)	96.74(11)	O(19)-V(7)-N(1)	91.09(17)
O(5)#1-V(2)-F(1)#1	74.42(9)	O(15)-V(5)-O(16)#1	102.44(14)	O(14)-V(7)-N(1)	158.67(13)
O(7)#1-V(2)-F(1)#1	79.75(8)	O(6)#1-V(5)-O(16)#1	84.41(11)	O(5)-V(7)-N(1)	80.91(13)
O(11)-V(3)-O(13)	106.0(1)				

Symmetry codes: #1: $-x$, $-y$, $-z$.

1.3 Calculation details

The DFT theory level of DMol3 code[23-26] was employed to calculate the geometry, electronic density, frontier orbital, and charge population of the $[V_{14}O_{36}F_2L_2]^{6-}$ anion and relative 2e oxidation species, $[V_{14}O_{36}F_2L_2]^{4-}$, using the X-ray geometric data, and spin unrestricted/restricted open/close-shell system as input data. Other options for the optimization were as follows: functional DFT exchange-correlation potential functional, *i.e.* the PWC local potential (LDA); basis DND; pseudopotential ECP; integration grid medium; charge −6/−4; multiplicity auto; quality medium. The counter ion, HL^+ cation, and lattice water are neglected. All calculations were performed on a commercial Dell precision computer.

2 Results and discussion

The monoclinic solid of **1** contains $[V_{14}O_{36}F_2L_2]^{6-}$ anion, HL^+ cation[27-28] and lattice waters (Fig.1), which are linked each other by way of complicated inter-molecular hydrogen bondings: N6…O12#1 (Symmetry codes: #1: $-x$, $-y+1$, $-z+1$; 0.290 6 nm), N6…O11#2 (Symmetry codes: #2: x, $-y+1/2$, $z+1/2$; 0.298 6 nm), N4…O9#3 (Symmetry codes: #3: $-x+1$, $y+1/2$, $-z+1/2$; 0.264 1 nm), N8…O10#4 (Symmetry codes: #4: $x+1$, $-y+3/2$, $z+1/2$; 0.287 3 nm), N8…O13#5 (Symmetry codes: #5: $-x+1$, $y+3/2$, $-z+1/2$; 0.308 2 nm), O1W…O19 (0.339 3 nm), O1W…O15#6 (Symmetry codes: #6: x, $y+1$, z; 0.287 8 nm), O2W…O18#7 (Symmetry codes: #7: x, y, $z+1$; 0.274 6 nm), O2W…O2W#8 (Symmetry codes: #8: $-x+1$, $-y+1$, $-z+2$; 0.274 3 nm). The offset and head-to-end π-π stacking interaction with an inter-plane distance of *ca.* 0.345 nm between adjacent imidazole rings of protonated HL^+ cations can also be observed. Both the former and latter contribute the stability of the crystalline solid.

The $[V_{14}O_{36}F_2L_2]^{6-}$ anion is centrosymmetrical, and contains four types of vanadium polyhedra. Two trimers of edge-sharing VO_5F octahedra form the heart of the polyanion. In each trimer, the vertex shared by the three octahedra is fluorine, which is characterized by bond valence analysis (0.72, close to theoretical

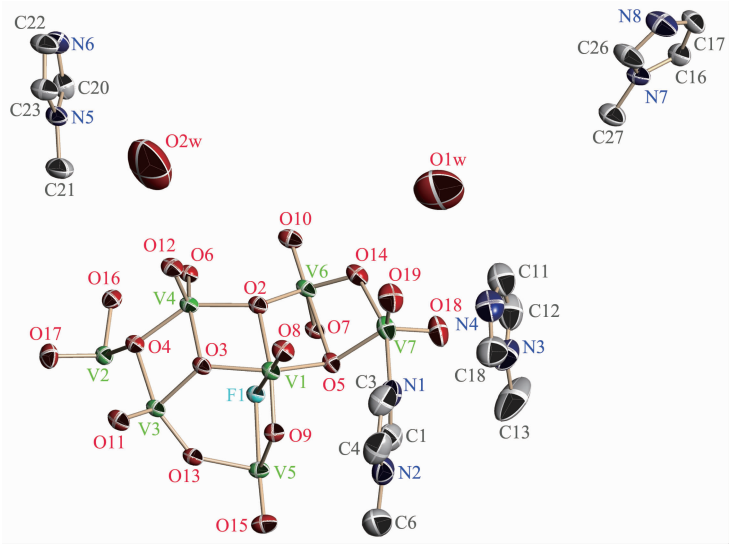

V: green, O: red, N: blue, F: light blue, C: gray

Fig.1　Perspective view of the unsymmetrical unit of crystalline **1** with 50% probability thermal ellipsoids

value 1 of F atom). Four VO_5 square pyramids bridge the two trimers via vertex-sharing μ_2-O and edge-sharing μ_3-O atoms. On the external side of each trimer, one VO_5 and one VO_4N trigonal bipyramids are grafted by way of μ_3-O and μ_4-O atoms, while in the axial direction of VO_4N trigonal bipyramid the V-N bonding interactions locate between V center and organic L ligand.

The connection between the six VO_5F octahedrons, four VO_5 square pyramids and four VO_5/VO_4N trigonal bipyramids of $[V_{14}O_{36}F_2L_2]^{6-}$ anion is very complicated, as the bridging O atoms are very diversities (containing μ_2-O, μ_3-O and μ_4-O atoms). Moreover there are terminal μ_1-O atoms per V centers, and organic ligands (L) scattering on the face of the shell-shaped cluster anion.

For the $[V_{14}O_{36}F_2L_2]^{6-}$ anion, a 0D ring-like ladder-chains cluster skeleton frame geometry, *i.e.* the $[V_{10}O_{20}]$ ladder (Fig.2), can be easily found, together with two VO_5F fragments of octahedral grafted above and below the $[V_{10}O_{20}]$ ladder, and two VO_3L fragments of trigonal bipyramidal located on the two sides of the $[V_{10}O_{20}]$ ladder. These core ring-like $[V_{10}O_{20}]$ ladder and grafted VO_5F and VO_3L fragments around the ladder are arranged in a centrosymmetric style. A possible self-assembling process of $[V_{14}O_{36}F_2L_2]^{6-}$ anion from core $[V_{10}O_{20}]$ ladder, grafted VO_5F and VO_3L fragments is roughly depicted in Fig.2. It is noted that the decomposition into core $[V_{10}O_{20}]$ ladder, and grafted VO_5F and VO_3L fragments may be arbitrary and not secret, but the theoretical importance and effect of electronic structure of these fragment

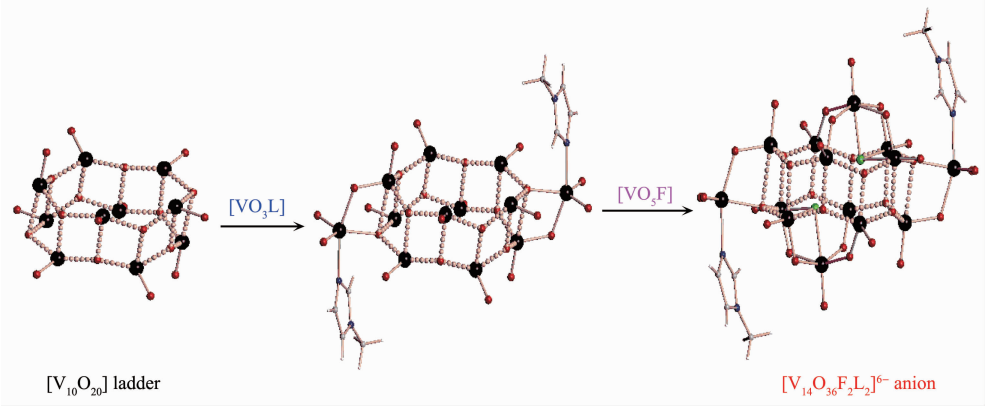

Fig.2　Self-assembling process of $[V_{14}O_{36}F_2L_2]^{6-}$ anion from a ring-like $[V_{10}O_{20}]$ ladder, two grafted $[VO_5F]$ and $[VO_3L]$ fragments

compositions will be clearly shown in later discussion.

Bond valence sum calculations indicate very interesting situation for the $[V_{14}O_{36}F_2L_2]^{6-}$ anion, as the valence state of all ten V centers of the $[V_{10}O_{20}]$ ladder to be +5, while those of the four V centers grafted to the ladder to be +4.4~4.6, which is in agreement with the charge balance, and the previous observation of the ladder-like chains structures of vanadium oxide cluster compounds being +5 valence state. However the valence state of *ca.* +4.5 for V centers is vague and unacceptable. The reasonable value of V centers is +4 or +5, an indicative that the four grafted V centers are probably mixed-valence.

The presence of fluorine in a vanadium oxide polyanionic compounds is often observed, generally as encapsulating inside the polyanion. The fluorine atoms should play the role of template for the self-assembling process of final cluster-like polyoxofluoro-vanadate compounds. However, the coordination of two organic L ligands into the surface of the vanadium oxide polyanionic cluster are rarely observation. The introduction of organic ligands will obviously change the electronic structure, and therefore tune the physical and chemical properties. The $[V_{14}O_{36}F_2L_2]^{6-}$ anion may be, as it were, a potentially important polyoxofluorovanadate functional material.

DFT-based theoretical calculations of Dmol3 module for $[V_{14}O_{36}F_2L_2]^{6-}$ anion shows interesting result. For comparison its 2e oxidation species $[V_{14}O_{36}F_2L_2]^{4-}$ anion was also calculated. These results of electron population analysis clearly show that two d^1 electrons of V (+4) centers of $[V_{14}O_{36}F_2L_2]^{6-}$ anion populate on the grafted VO_5F fragments, while the grafted VO_3L fragments are away from those *d* electrons (Fig.3), an indicative that the former is +4 oxidation state and the latter +5 oxidation state for vanadium centers. The d electrons are moderately delocated over four μ_2-oxo-linking V centers of the $[V_{10}O_{20}]$ ladder, which may interpret the observation fact of the two grafted VO_5F fragments being *ca.* +4.5 in bond valence sum calculation. While the abnormity of observed bond valence sum of V centers (+5 oxidation state) of the grafted VO_3L fragments may be ascribed to the large steric effect from adjacent big $[V_{10}O_{20}]$ ladder and L ligand, which decrease the bond valence value of V centers.

A comparison of frontier orbitals of $[V_{14}O_{36}F_2L_2]^{6-}$ and relative 2e oxidizing anion, $[V_{14}O_{36}F_2L_2]^{4-}$ (Fig.3), indicates very interesting phenomenon. For the latter the HOMO is *d-p* π orbital between V centers and terminal O atoms of grafted VO_3L fragments, while the LUMO and LUMO+1 *d* orbitals of V centers of grafted VO_5F fragments with moderate charge delocalization over four V atoms of the $[V_{10}O_{20}]$ ladder. The chemical

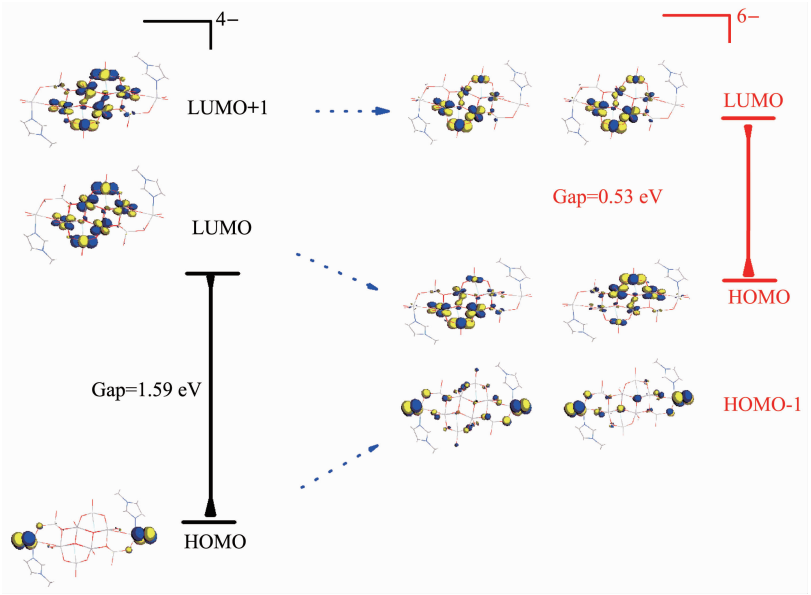

Fig.3 Calculated frontier orbital energy levels and diagrams of $[V_{14}O_{36}F_2L_2]^{6-}$ and relative $[V_{14}O_{36}F_2L_2]^{4-}$ anion

property of $[V_{14}O_{36}F_2L_2]^{4-}$ anion should be associated with the terminal V=O (*d-p*) π orbital of grafted VO_3L fragments. The energy gap of LUMO-HOMO is *ca.* 1.59 eV. However it greatly decreases to *ca.* 0.53 eV after a 2e reduction to $[V_{14}O_{36}F_2L_2]^{6-}$ anion, indicating that the $[V_{14}O_{36}F_2L_2]^{6-}$ anion is more excellent semiconductor in conductivity. After the 2e reduction the HOMO, LUMO and LUMO+1 in $[V_{14}O_{36}F_2L_2]^{4-}$ become HOMO-1, HOMO and LUMO of $[V_{14}O_{36}F_2L_2]^{6-}$, respectively (Fig.3). Now please note that the frontier HOMO, namely d orbital of grafted VO_5F fragments, being moderate delocalization over other V centers of the $[V_{10}O_{20}]$ ladder contributes greatly to the small energy gap, and therefore, more excellent conductivity of $[V_{14}O_{36}F_2L_2]^{6-}$ anionic semiconducting material than $[V_{14}O_{36}F_2L_2]^{4-}$ anionic semiconducting material can be expected. Owing to HOMO being of *d* orbital of grafted VO_5F fragments the solid material of $[V_{14}O_{36}F_2L_2]^{6-}$ anion should be chemically active for *d* electron of V centers, which is wholly different from the case of $[V_{14}O_{36}F_2L_2]^{4-}$ anionic material.

Let us look into in detail the diagrams of frontier orbital, the additional two electrons will occupy the LUMO or LUMO+1 orbital of $[V_{14}O_{36}F_2L_2]^{4-}$ anion and become the HOMO of $[V_{14}O_{36}F_2L_2]^{6-}$ anion. Though the 2e reduction process is not preferred in energy as the electrons will populate onto the anti-bonding LUMO or LUMO+1 orbital of $[V_{14}O_{36}F_2L_2]^{4-}$ anion, this process will lead obviously the increasing structural stability of the skeleton frame of core $[V_{10}O_{20}]$ ladder and simultaneously activate the grafted VO_5F and VO_3L fragments (this can be easily seen from the frontier orbital). In other words, the special geometry (including core $[V_{10}O_{20}]$ ladder, and grafted VO_5F and VO_3L fragments) and interesting electronic figuration of $[V_{14}O_{36}F_2L_2]^{6-}$ anion ensure that this anionic material has a stronger core $[V_{10}O_{20}]$ ladder skeleton frame, and more active grafted VO_5F and VO_3L fragments, which will dominate the chemical and physical properties and improve the behavior as inorganic functional solid. It is concluded that $[V_{14}O_{36}F_2L_2]^{6-}$ anionic material, to some extent should be very special in including semiconducting property, catalytic property and chemical reactivity. Therefore it is valuable to further investigate it theoretically and experimentally, and we'll pay much attention to it in our laboratory in the future.

3 Conclusions

In summary, a rare tetradecanuclear polyoxofluorovanadate cluster with 1-methylimidazole (L), containing $[V_{14}O_{36}F_2L_2]^{6-}$ anion, was synthesized and characterized by X-ray diffraction method. The anion is decomposed into a special core of 0D ring-shaped cluster-like skeleton frame, *i.e.* the $[V_{10}O_{20}]$ ladder, and two grafted VO_5F and VO_3L fragments are around the ladder core. DFT theoretical and bond valence sum calculations of $[V_{14}O_{36}F_2L_2]^{6-}$, indicated that the grafted VO_5F fragments are V(+4) oxidation state, while other V centers are V(+5) oxidation state. The frontier orbital analyses showed that $[V_{14}O_{36}F_2L_2]^{6-}$ anion, should be chemically active in *d* orbital of grafted VO_5F fragments, while its 2e oxidation species, the $[V_{14}O_{36}F_2L_2]^{4-}$ anion should be chemically active in the terminal V=O (*d-p*) π orbital of grafted VO_3L fragments. The 2e reduction from $[V_{14}O_{36}F_2L_2]^{4-}$ to $[V_{14}O_{36}F_2L_2]^{6-}$ anion, being unfavorable in energy, but leads to the increasing structural stability of the core $[V_{10}O_{20}]$ ladder, and at the same time the increasing activity of the grafted VO_5F and VO_3L fragments, together with a great decrease of energy gap (from 1.59 to 0.53 eV). Based on the special electron structure, the $[V_{14}O_{36}F_2L_2]^{6-}$ anionic materials may be quite important candidates of potential applications in semiconducting industry catalytic materials and chemical reactivity. It is valuable to further investigate it theoretically and experimentally in the future.

Acknowledgments: This work was supported by the Foundation for Research Group of Inorganic Solid Functional Materials (Grant No.2015KCXTD030), the National Natural Science Foundation of China (Grant No.21271080), the foundation of Research and Development Center of Green chemical Engineering and Functional Materials of Guangdong Provincial Universities, and the Science and Technology Planning Project of Huizhou City, Guangdong Province, China (Grant No. 2012B020004006), which are gratefully acknowledged.

References:

[1] Baker L C W, Glick D C. *Chem. Rev.*, **1998**,**98**:3-50

[2] Sessoli R, Tsai H L, Schake A R, et al. *J. Am. Chem. Soc.*, **1993**,**115**:1804-1816

[3] Müler A, Peters F, Pope M T, et al. *Chem. Rev.*, **1998**,**98**: 239-272

[4] Nishio M, Inami S, Katayama M, et al. *Inorg. Chem.*, **2012**, **51**:784-793

[5] Raghu C, Rudra I, Ramasesha S, et al. *Phys. Rev. B*, **2000**, **62**:9484-9493

[6] HE Miao(贺淼), JIAO Qing-Zhu(焦庆祝), CHEN Xiang-Fei (陈相飞), et al. *Chinese J. Inorg. Chem.*(无机化学学报), **2015**,**31**(8):1590-1596

[7] GUO Jiu-Yu(郭九玉), ZHANG Zhi-Bin(张志斌), YAN Da-Wei(颜大伟), et al. *Chinese J. Inorg. Chem.*(无机化学学报), **2011**,**27**(10):2100-2104

[8] Gatteschi D, Sessoli R. *Angew. Chem. Int. Ed.*, **2003**,**42**:268 -297

[9] Gouzerh P, Proust A. *Chem. Rev.*, **1998**,**98**:77-112

[10]Hagrman P J, Hagrman D, Zubieta J. *Angew. Chem. Int. Ed.*, **1999**,**38**:2638-2803

[11]Regnault N, Jolicoeur, Sessoli R, et al. *Phys. Rev. B*, **2002**, **66**:054409

[12]Hegetschweiler K, Morgenstern B, Zubieta J, et al. *Angew. Chem. Int. Ed.*, **2004**,**43**:3436-3439

[13]Yang W, Lu C. *Inorg. Chem.*, **2002**,**41**:5638-5640

[14]Spandl J, Brüdgam I, Hartl H. *Angew. Chem. Int. Ed.*, **2001**, **40**:4018-4020

[15]Zhao Y, Zhu G, Liu W, et al. *Chem. Commun.*, **1999**:2219-2220

[16]Ninclaus C, Riou D, Férey G. *Chem. Commun.*, **1997**:851-852

[17]Shi Z, Zhang L, Zhu G, et al. *Chem. Mater.*, **1999**,**11**:3565-3570

[18]Tong Y P, Luo G T, Zhou W, et al. *Inorg. Chem. Commun.*, **2010**,**13**:1281-1284

[19]Tong Y P, Luo G T, Jin Z, et al. *Aust. J. Chem.*, **2011**,**64**: 973-977

[20]Tong Y P, Liu H, Jin Z, et al. *Monatsh. Chem.*, **2012**,**143**: 1005-1010

[21]Blessing R H. *Acta Crystallogr. Sect. A*: *Found. Crystallogr.*, **1995**,**A51**:33-38

[22]Sheldrick G M. *SHELXTL* 6.10, *Bruker Analytical Instrumentation*, Madison, Wisconsin, USA, **2000**.

[23]Delley B. *J. Phys. Chem. A*, **2006**,**110**:13632-13639

[24]Delley B. *J. Phys.*: *Condens. Matter.*, **2010**,**22**:384208

[25]Delley B. *J. Chem. Phys.*, **1990**,**92**:508-517

[26]Delley B. *J. Chem. Phys.*, **2000**,**113**:7756-7764

[27]Siddiqi Z A, Anjuli, Sharma P K, et al. *J. Mol. Struct.*, **2012**, **1029**:86-91

[28]Mestroni G, Alessio E, Santi A S, et al. *Inorg. Chim. Acta*, **1998**,**273**:62-71